Talanta 127 (2014) 146–151

Contents lists available at ScienceDirect

Talanta

journal homepage: www.elsevier.com/locate/talanta

Evaluation of the plasticization of ion-selective electrode membranes by pulsed NMR analyses

Takayo Moriuchi-Kawakami [a,*], Yuki Kanaya [a], Yoshiaki Urahama [b]

[a] Department of Applied Chemistry, Faculty of Engineering, Osaka Institute of Technology, 5-16-1 Omiya, Asahi, Osaka 535-8585, Japan
[b] Graduate School of Engineering, University of Hyogo, 2167 Shosha, Himeji, Hyogo 671-2201, Japan

ARTICLE INFO

Article history:
Received 22 February 2014
Received in revised form
2 April 2014
Accepted 3 April 2014
Available online 15 April 2014

Keywords:
Pulsed NMR
Proton spin–spin relaxation time T_2
Potentiometric polymeric membrane
Plasticization
Ion-selective electrode (ISE)

ABSTRACT

The potentiometric polymeric membranes for ion-selective electrodes were evaluated by analyses of the proton spin–spin relaxation times T_2 with pulsed NMR. The T_2 measurements were performed using the Hahn-Echo, Solid-Echo and CPMG pulse sequences. The T_2 values and fractions F of each component were obtained by analyses of the FID signals measured with the Hahn-Echo pulse sequence. The softer potentiometric polymeric membrane possessed the main fraction F_L, providing a relatively longer T_{2L} value. A linear relationship existed between the weight ratio of the membrane solvent and $\ln T_{2L}$ (or ln total $T_2 \times F$). This analysis method could quantify the degree of hardness or softness of the potentiometric polymeric membranes with the differences in the membrane solvent weight. The normalized derivative spectra were acquired from the transverse magnetization $M(t)$ data measured by using the Solid-Echo and CPMG pulse sequences. In the normalized derivative spectra of the potentiometric polymeric membranes, most PVC peaks in the short time region shifted to a larger area of long time regions by plasticization, and the softer potentiometric polymeric membrane incorporating more membrane solvent exhibited a relaxation peak in the relatively longer time region. Thus, the normalized derivative spectra were effective in elucidating the compatibility of the PVC with the membrane solvent.

1. Introduction

Ion-selective electrodes (ISEs) form one of the most important groups of chemical sensors [1–3]. Moreover, solvent polymeric membrane electrodes are attractive due to the facile design of their novel ionophores as analytical agents. An ionophore, which is dissolved or dispersed in a potentiometric polymeric membrane, actually discriminates ions. A typical potentiometric polymeric membrane for ISEs is composed of 1–7 wt% ionophore, 30 wt% poly(vinyl chloride) (PVC) as the polymer, 66–67 wt% membrane solvent, and 1–2 wt% salt additive [4,5]. Although ionophores mainly discriminate ions in a potentiometric polymeric membrane, all the components of ISEs influence their ion-sensing behavior [4]. Therefore, the properties of not only the individual components but also the entire membrane matrix appear to be quite critical to the ion-sensing behavior of ISEs. Among the various physical properties of ISEs such as impedance, membrane resistance, dielectric constant and ionic conductivity, etc., plasticization (i.e., the hardness or softness and compatibility with the membrane solvent) of the potentiometric polymeric membranes will particularly affect their ion-sensing behavior. Nevertheless, a suitable and valid analysis method to evaluate the plasticization of potentiometric polymeric membranes has yet to be developed.

Nuclear magnetic resonance (NMR) analysis has provided considerable insight into molecular relaxation in various morphological domains and the ways in which it influences the overall macroscopic properties of polymers [6]. Pulsed NMR analyses [7] can also quickly determine the spin–lattice (T_1) and spin–spin (T_2) relaxation times [8–20]. In fact, in recent times, the evaluation of various materials using T_2 measurements has been widely applied in various scientific fields [21–27]. The study of T_2 can, thus, be considered a useful tool in elucidating the properties of potentiometric polymeric membranes. We have previously demonstrated that the difference in hardness or softness of plasticized potentiometric polymeric membranes by different membrane solvents appears in the sum of the product of the T_2 value and its fraction F value (total $T_2 \times F$) acquired by pulsed NMR analysis [28]. It was the first report on the characterization of potentiometric polymeric membranes for ISEs using T_2 data obtained from pulsed NMR investigations. However, the total $T_2 \times F$ value merely indicated a rough degree of their hardness or softness due to the difference in the membrane solvents.

---

[*] Corresponding author. Tel./fax: +81 6 6954 4281.
E-mail address: kawakami@chem.oit.ac.jp (T. Moriuchi-Kawakami).

http://dx.doi.org/10.1016/j.talanta.2014.04.006

In this study, plasticization of potentiometric polymeric membranes incorporating the same membrane solvent is investigated. Evaluations with pulsed NMR analyses were carried out by applying three pulse sequences, the first being the same pulse sequence used in a previous study [28]. The Hahn-Echo pulse sequences [7] were applied, and this 90°–τ–180° pulse sequence was suitable in obtaining FID signals for the T_2 values and its fraction F value of the viscoelastic electrode membranes. The second and third pulse sequences were utilized for the normalized derivative spectra. The Solid-Echo [29] and Carr–Purcell–Meiboom–Gill (CPMG) [30,31] pulse sequences were applied, and the 90°–τ–90° and 90°–τ–$\{[180^\circ$–2τ–$]_M$ $180^\circ - \tau -$ measurement $- \tau\}_N$ pulse sequences were suitable to obtain transverse magnetization $M(t)$ data from the short time region to the long time region for the normalized derivative spectra. Such $M(t)$ data may include much information on the components and molecular motions, however, it is actually too difficult to find such information from the $M(t)$ data. We have succeeded in acquiring the normalized derivative spectra by derivative calculations of the $M(t)$ data with respect to the logarithmic time [32]. In fact, the normalized derivative spectra clearly depicted the differences in plasticization.

2. Experimental

2.1. Reagents

All reagents were commercially available and used as such unless otherwise specified. Tetrahydrofuran (THF) was dried over sodium and distilled.

2.2. Preparation of ion-selective electrode membranes

The basic potentiometric polymeric membrane, as a potentiometric cation-sensing membrane, is composed of PVC (27.9 wt%) as the polymer, 2-nitrophenyl octyl ether (*o*-NPOE) (68.5 wt% I'm) as a membrane solvent, 5,10,15,20-tetraphenyl porphyrin (**TPP**) (2.5 wt%) as an ionophore, and potassium tetrakis(4-chlorophenyl) borate (KTpClPB) (0.6 wt%) as an anion excluder [33]. The components were placed into a 5 mL glass tube and dissolved in ca. 3 mL of THF. The PVC plasticized membrane was obtained by spontaneous evaporation of THF for a few days. Five kinds of potentiometric polymeric membranes with differences in their membrane solvent weight were prepared by the same procedure. The weight ratios of *o*-NPOE as a membrane solvent were altered from 58.5 wt % to 78.5 wt%, although the total weight of the PVC and *o*-NPOE was kept constant (96.5 wt%).

2.3. Pulsed NMR measurements and evaluations

Pulsed NMR measurements were carried out with a JEOL JNM-MU-25 spectrometer operating at a frequency of 25 MHz. One sheet of each type of potentiometric polymeric membrane mentioned above was arranged in a 10 mmϕ NMR tube for pulse irradiation to its center. Digital images of these five types of membranes before pulsed NMR measurements are shown in Fig. S1 of the Supplementary materials. The free induction decay (FID) signals were recorded at a probe temperature of 25 °C. The spin–spin relaxation time T_2 values were estimated by the Hahn-Echo method (90°–τ–180° pulse sequence). The T_2 values and the fraction of each component were calculated by fitting the FID signal to the Weibull function [34], while the T_2 values were also estimated by the Solid-Echo (90°–τ–90° pulse sequence) and Carr–Purcell–Meiboom–Gill (90°–τ–$\{[180^\circ$–2τ–$]_M$ 180°–τ–measurement–$\tau\}_N$ pulse sequence) methods. Likewise, the FID signals were recorded at a probe temperature of 25 °C. FID signals for different measurement ranges were collected to obtain high-accurate transverse magnetization $M(t)$ data and the normalized derivative spectra.

2.4. EMF measurements and evaluations

The potentiometric polymeric membrane was formed on the tip of the ISE body assembly with an electrode kit (DKK Co. Ltd., Tokyo) by a casting method. The obtained solvent polymeric membrane electrodes were then conditioned overnight in an aqueous 0.01 M $AgNO_3$ solution. EMF measurements were performed on cells of type Ag–AgCl | 0.1 M $AgNO_3$ ‖ membrane ‖ sample solution | 0.1 M CH_3COOLi ‖ 3.3 M KCl | AgCl–Ag using a pH/mV meter equipped with a double junction type Ag–AgCl reference electrode. The activity coefficients were calculated according to the Davies equation [35]. EMF measurements of the solvent polymeric membrane electrodes were carried out in increasing $AgNO_3$ concentrations at 25 °C. The selectivity coefficients of the five ISEs were determined by the fixed interference method (FIM) [2].

3. Results and discussion

3.1. Pulsed NMR studies with the Hahn-Echo pulse sequence

The hardness or softness and compatibility of a membrane solvent in a polymer or the entanglement of a polymer vary as the weight ratio or the kind of employed membrane solvent is changed [36]. When the same membrane solvent is employed as a plasticizer, the direction of hardness or softness for the potentiometric polymeric membrane can be quantitatively shaped by the weight ratio of the membrane solvent. Likewise, the T_2 value of the potentiometric polymeric membrane is dramatically affected by the weight ratio of the employed membrane solvent since constraints on the molecular motions in the potentiometric polymeric membrane are directly influenced by their hardness or softness. To estimate the degree of hardness or softness of the potentiometric polymeric membrane, their T_2 values were acquired by analyses of the free induction decay (FID) signals measured at 25 °C using a pulsed NMR spectrometer operating at a frequency of 25 MHz. Fig. 1 shows the FID signals of the five potentiometric polymeric membranes incorporating *o*-NPOE measured by using the Hahn-Echo 90°–τ–180° pulse sequence.

The proton spin–spin relaxation times T_2 and the fraction of each component were calculated by fitting the FID signal to the Weibull function [34]. Each FID signal of the potentiometric polymeric membranes examined offered the relaxation times T_{2L}

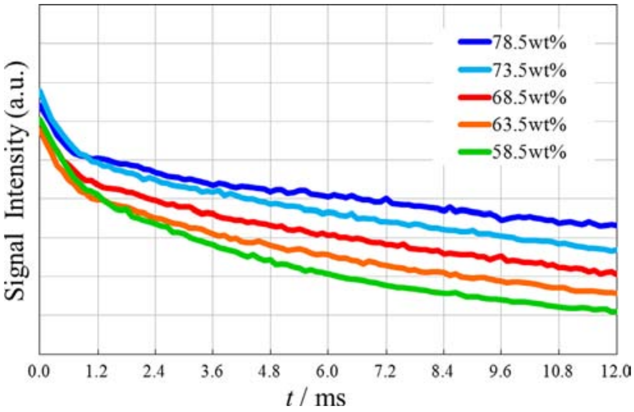

Fig. 1. The FID signals with the Hahn-Echo pulse sequence of five potentiometric polymeric membranes incorporating *o*-NPOE as a membrane solvent.

(long) and T_{2M} (intermediate) [19], indicating that each fraction of the different T_2 belongs to a different mobility region by plasticization. The longer T_{2L} and the shorter T_{2M} are attributed to a mobile species and loosely entangled polymer, respectively. The T_2 values and their respective fractions F are summarized in Table 1.

The softer potentiometric polymeric membranes incorporating more *o*-NPOE possessed a larger fraction F_L, providing a longer T_{2L} value. The softest membrane incorporating 78.5 wt% of *o*-NPOE possessed the major fraction F_L (81.5%), providing the longest T_{2L} value (27.12 ms). It is noteworthy that the degree of hardness or softness of the membranes is quantitatively exhibited in the T_2 values of the major fractions F; linear increases in the weight ratios of the *o*-NPOE employed were accompanied by exponential increases in the T_{2L} values of the major fractions F. Likewise, the linear increases in the weight ratios of *o*-NPOE were also accompanied by exponential increases in the sum of the product of a T_2 value and its F value, namely the total $T_2 \times F$ values (see Fig. S2). The total $T_2 \times F$ value expresses the average of the obtained T_2 values. The plots for the weight ratio of *o*-NPOE vs $\ln T_{2L}$ (or the ln total $T_2 \times F$) give a straight line, as shown in Fig. 2. Considered with previous results [28], it was evidently demonstrated that the total $T_2 \times F$ values could exhibit the degree of the relatively mobile region for the potentiometric polymeric membranes, thus reflecting the degree of hardness or softness of the entire membrane matrix. The Hahn-Echo pulse sequence rather than the Solid-Echo and CPMG pulse sequences was found to be suitable in acquiring the T_2 values of the viscoelastic electrode membranes.

Table 1
Result of spin–spin relaxation time T_2 measurements by pulsed NMR.

NPOE (wt%)	FID graphs[a]				Total $T_2 \times F$ (ms)
	T_{2M} (μs)	F_M (%)	T_{2L}(ms)	F_L (%)	
58.5	737	29.1	8.39	70.9	6.2
63.5	503	24.8	11.39	75.2	8.7
68.5	604	20.5	14.97	79.5	12.0
73.5	627	22.9	19.61	77.1	15.3
78.5	518	18.5	27.12	81.5	22.2

[a] Estimated from a Hahn-Echo FID signal.

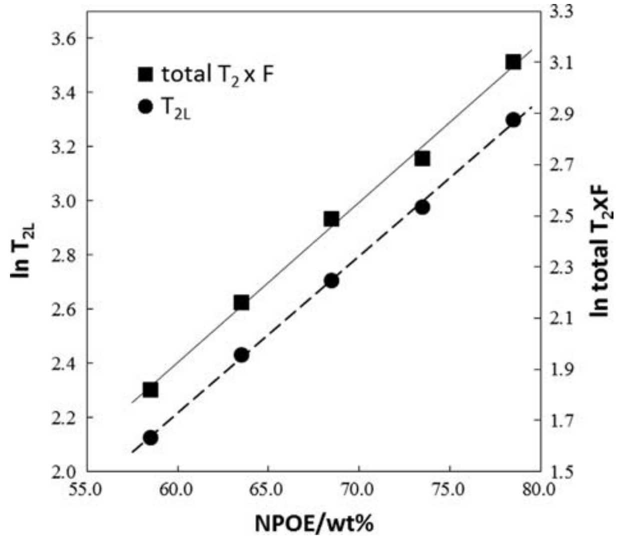

Fig. 2. Changes of $\ln T_{2L}$ and ln (total $T_2 \times F$) values with the weight ratios of *o*-NPOE as the membrane solvent.

3.2. Pulsed NMR studies with the Solid-Echo and CPMG pulse sequences

In order to acquire the normalized derivative spectra, the FID signals were measured by pulsed NMR with the Solid-Echo and CPMG pulse sequences. The high-accurate transverse magnetization $M(t)$ data was given by a modification in the measurement range. One item of $M(t)$ data was gleaned from several FID signals and smoothed, acquiring the normalized derivative spectra by derivative calculations with respect to the logarithmic time. The transverse magnetization $M(t)$ is expressed by the following equation, where τ_i is the relaxation time, m_i is the Weibull coefficient and a_i is the intensity factor of the *i*-th component [37]:

$$M(t) = \sum(a_i \times \exp(-t/\tau_i)^{m_i})$$

Fig. 3 illustrates the $M(t)$ data of five potentiometric polymeric membranes incorporating *o*-NPOE with differences in weight ratio measured with the Solid-Echo and CPMG pulse sequences in the time range of 1 μs to 20,000,000 μs. Furthermore, the $M(t)$ data of PVC employed as a polymer and *o*-NPOE as the membrane solvent for the membranes were included. The scale of the horizontal axis is logarithmic. The remarkable difference between potentiometric polymeric membranes and PVC was clearly observed in the $M(t)$ data. The T_2 relaxation of PVC appeared only in short time regions up to 100 μs. On the other hand, the T_2 relaxations of potentiometric polymeric membranes were found in a wider field of long time regions of 100 μs to 200,000 μs. Although the potentiometric polymeric membranes incorporated PVC by weight ratio from 18 wt% to 38 wt%, they scarcely showed properties of the original PVC in the $M(t)$ data. These results establish that when PVC is plasticized by the membrane solvent *o*-NPOE, the constraints on the molecular motions of PVC are dramatically reduced. Furthermore, these $M(t)$ data for the potentiometric polymeric membranes were different from those for *o*-NPOE. However, between the potentiometric polymeric membranes, differences in the $M(t)$ data, except for the intensity factor a_i, were difficult to confirm.

Fig. 4 shows the normalized derivative spectra in the time range of 1 μs to 20,000,000 μs for the five potentiometric polymeric membranes incorporating the membrane solvent *o*-NPOE with differences in weight ratio. The normalized derivative spectra of PVC and the membrane solvent *o* -NPOE are also illustrated in Fig. 4. The data $S(t)$ for the normalized derivative spectra was calculated by derivation calculations of $M(t)$ with respect to the logarithmic time. The data $S(t)$ for the normalized derivative spectra is expressed with the following equation:

$$S(t) = d\,M(t)/d \ln t$$

Each peak, referred to as a relaxation peak, shows the time when relaxation occurred. The remarkable difference between potentiometric polymeric membranes and PVC is clearly depicted in the normalized derivative spectra. The relaxation peaks of PVC appeared in the short time region up to 30 μs. However, in the normalized derivative spectra of the potentiometric polymeric membranes, such relaxation peaks of PVC were slightly detected. These results clearly indicate that a considerable blending of the PVC into the membrane solvent *o*-NPOE occurs and that constraints on the molecular motions of PVC are substantially reduced by plasticization. Most PVC peaks in the short time region shifted to a wider field of long time regions by plasticization. The large relaxation peaks of the potentiometric polymeric membranes appeared around the time region of 10,000 μs. The softer potentiometric polymeric membrane incorporating more membrane solvent exhibited a relaxation peak in the relatively longer time region.

Surprisingly, the normalized derivative spectra of all the potentiometric polymeric membranes resembled those of the

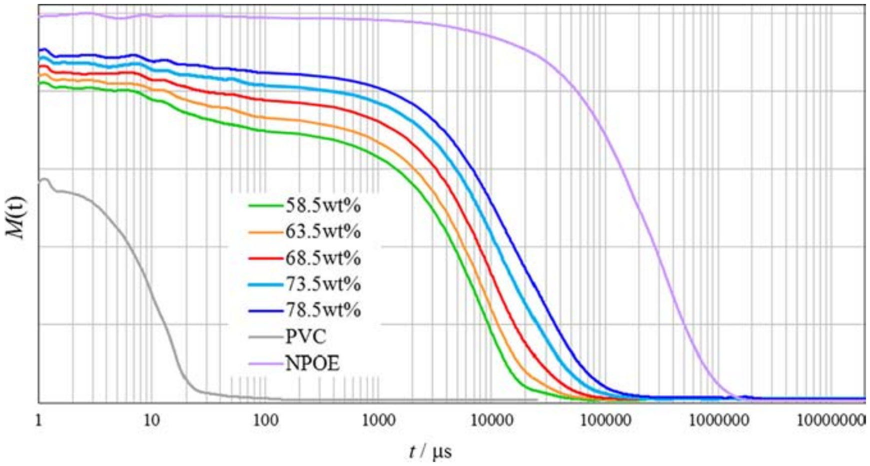

Fig. 3. Time dependence of the transverse magnetizations $M(t)$ with the logarithmic time.

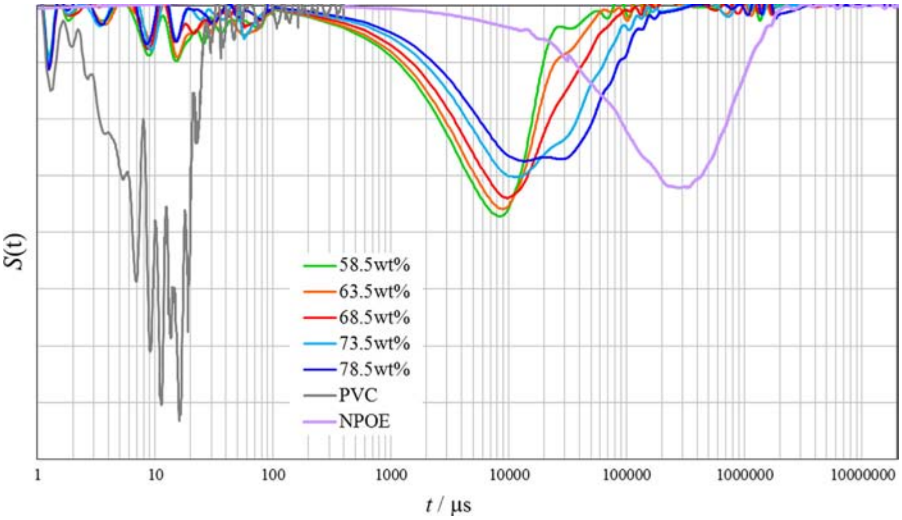

Fig. 4. Normalized derivative spectra of the potentiometric polymeric membranes incorporating *o*-NPOE as the membrane solvent.

membrane solvent *o*-NPOE rather than PVC: the large relaxation peaks of *o*-NPOE appeared around the time region of 300,000 μs. The ion-sensing behaviors of the potentiometric polymeric membranes are influenced by the membrane solvents since such physical properties greatly depend on the membrane solvents employed. The differences among the membranes are also clearly characterized in the normalized derivative spectra. The times which provide the minimum $S(t)$ values in the normalized derivative spectra are observed to shift depending on the weight ratios of the membrane solvent *o*-NPOE. The hardest potentiometric polymeric membrane incorporating 58.5 wt% of *o*-NPOE possessed the minimum $S(t)$ value at the shorter time 8400 μs. The softest potentiometric polymeric membrane incorporating 78.5 wt% of *o*-NPOE possessed the minimum $S(t)$ value at the longer time 13,600 μs. The membrane solvent *o*-NPOE possessed the minimum $S(t)$ value at the longest time of 280,000 μs. Namely, the constraints on the molecular motions of PVC were noticeably reduced by plasticization, while the constraint on the molecular motions of *o*-NPOE were also markedly increased. These results suggest that the compatibility of PVC with the membrane solvent is increased by the increase in the weight ratio of the membrane solvent *o*-NPOE.

In the data $S(t)$ of the potentiometric polymeric membranes, the peaks around the time region of 30,000 μs were gradually appeared with increasing in the weight ratios of the membrane solvent *o*-NPOE. Interestingly, the second peak with the minimum $S(t)$ value at 28,000 μs was clearly observed in the data $S(t)$ of the softest potentiometric polymeric membrane incorporating 78.5 wt % of *o*-NPOE. It seems that the second peak is attributed to the molecular motion of the *o*-NPOE which is poorly compatible with PVC and the appearance of the peak indicates the presence of a little excess of the membrane solvent.

3.3. Potentiometric studies

To investigate the influence of plasticization on the ion-sensing behaviors of the potentiometric polymeric membranes, the selectivity coefficients were obtained from EMF measurements of the ISEs. As shown in Fig. S3, all the solvent polymeric membrane electrodes displayed high sensitivity and fast potential response to the Ag^+ ion. The solvent polymeric membrane electrode incorporating 68.5 wt% of *o*-NPOE responded to the Ag^+ – activity changes with slopes of 57.7 mV decade^{-1} over the activity ranges of $10^{-4.5}$ to $10^{-1.1}$ M. The slopes and linear ranges of the calibration graph are summarized in Table S1. Fig. 5 illustrates the selectivity coefficients of five ISEs determined by the fixed interference method (FIM). The ion selectivity sequences were affected by the weight ratios of the *o*-NPOE employed. The ion-sensing behavior of the potentiometric polymeric membrane incorporating 68.5 wt % of *o*-NPOE was best. This result demonstrated that the increase–decrease change in the weight ratios of the membrane solvent will be effective for the improvement of the ion-sensing behavior.

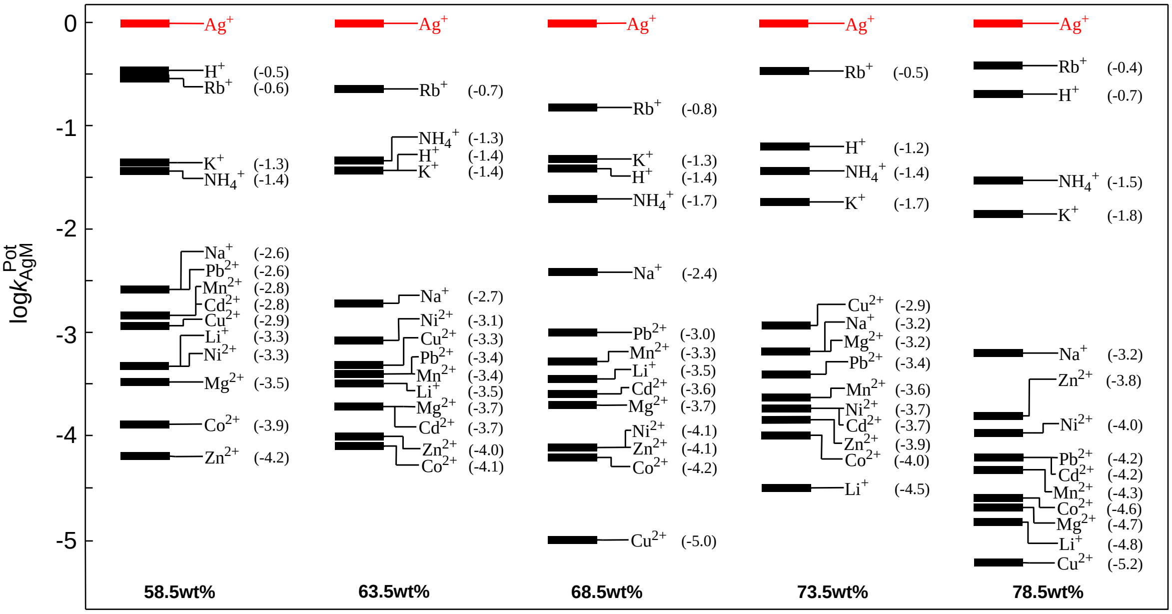

Fig. 5. Selectivity coefficients of potentiometric liquid membrane electrodes based on the porphyrin **TPP** (determined by the fixed interference method (**FIM**)).

However, it was indicated that the increase of the plasticization did not necessarily improve the ion-sensing behavior. This is because a little excess of the membrane solvent presumably influenced the ion-sensing behavior. The proposed normalized derivative spectra can illustrate the presence of a little excess of the membrane solvent. The change in ion selectivity depends on both the chemical and physical properties of the employed membrane solvent.

4. Conclusion

In summary, to obtain useful information on plasticization, the proton spin–spin relaxation times (T_2) of ion-selective electrode membranes with differences in membrane solvent weight were measured using a pulsed NMR spectrometer (with the Hahn-Echo, Solid-Echo and CPMG pulse sequences). We were able to demonstrate that the degree of plasticization for potentiometric polymeric membranes incorporating the same membrane solvent is quantitatively exhibited in the T_2 values of the major fractions F: a linear relationship was found to exist between the weight ratio of the membrane solvent and the $\ln T_{2L}$ (or $\ln$ total $T_2 \times F$). The T_2 measurements using the Hahn-Echo pulse sequences provided valuable information about the degree of plasticization for the ion-selective electrode membranes. Moreover, we demonstrated that the normalized derivative spectra acquired from the T_2 measurements using the Solid-Echo and CPMG pulse sequences remarkably characterized the differences among the potentiometric polymeric membrane in the compatibility of PVC with the membrane solvent. Thus, analysis of the normalized derivative spectra was seen to be a useful tool in elucidating the mechanisms behind the plasticization of potentiometric polymeric membranes.

Acknowledments

This study was supported by JSPS KAKENHI (Grant No. 25410155 to T. M.-K.).

Appendix A. Supplementary material

Supplementary data associated with this article can be found in the online version at http://dx.doi.org/10.1016/j.talanta.2014.04.006.

References

[1] E. Bakker, M.T. Diaz, Anal. Chem. 74 (2002) 2781–2800.
[2] E. Bakker, P. Bühlmann, E. Pretsch, Chem. Rev. 97 (1997) 3083–3132.
[3] E. Bakker, E. Pretsch, Angew. Chem. Int. Ed. 46 (2007) 5660–5668.
[4] Y. Umezawa, in: B. Raton, A. Arbor (Eds.), CRC Handbook of Ion-Selective Electrodes: Selectivity Coefficients, CRC Press, Boston, 1990.
[5] R.W. Cattrall, in: R.G. Compton (Ed.), Chemical Sensors, Oxford University Press Inc., Oxford/New York, Melbourne, 1997, pp. 13–23 (Chapter 3).
[6] V.J. Mcbrierty, D.C. Douglass, Phys. Rep. 63 (1980) 61–147.
[7] E.L. Hahn, Phys. Rev. 80 (1950) 580–594.
[8] T.J. Rowland, L.C. Labun, Macromolecules 11 (1978) 466–471.
[9] R. Folland, J.H. Steven, A. Charlesby, J. Polym. Sci. Polym. Phys. 16 (1978) 1041–1057.
[10] R. Folland, A. Charlesby, Polymer 20 (1979) 207–210.
[11] R. Folland, A. Charlesby, Polymer 20 (1979) 211–214.
[12] G.C. Munie, J. Jonas, J. Polym. Sci. Polym. Chem. 18 (1980) 1061–1070.
[13] D.R. Brown, G.C. Munie, J. Jonas, J. Polym. Sci. Polym. Phys. 20 (1982) 1659–1668.
[14] H. Tanaka, T. Nishi, J. Chem. Phys. 82 (1985) 4326–4331.
[15] H. Ohta, I. Ando, S. Fujishige, K. Kubota, J. Polym. Sci. Polym. Phys. 29 (1991) 963–968.
[16] N. Tanaka, S. Matsukawa, H. Kurosu, I. Ando, Polymer 39 (1998) 4703–4706.
[17] H. Kimoto, A. Asano, A. Fukuda, C.M. Sullivan, T. Kurotsu, Anal. Sci. 17 (2001) a155–a158.
[18] M. Kanekiyo, M. Kobayashi, I. Ando, H. Kurosu, S. Amiya, Macromolecules 33 (2000) 7971–7976.
[19] H. Kimoto, A. Fukuda, A. Asano, T. Kurotsu, Anal. Sci. 21 (2005) 315–319.
[20] D. Fairhurst, S. Prescott, Spectrosc. Eur. 23 (2011) 13–16.
[21] S. Mizukami, R. Takikawa, F. Sugihara, Y. Hori, H. Tochio, M. Wälchli, M. Shirakawa, K. Kikuchi, J. Am. Chem. Soc. 130 (2008) 794–795.
[22] G.M. Bosmans, B. Lagrain, L.J. Deleu, E. Fierens, B.P. Hills, J.A. Delcour, J. Agric. Food Chem. 60 (2012) 5461–5470.
[23] A.P. Birchenko, N.P. Mikhin, E.Y. Rudavskii, Y.O. Vekhov, J. Low Temp. Phys. 169 (2012) 208–217.
[24] C.I. Harvat, X. Zhu, D. Türp, R.A. Vinokur, D.E. Demco, R. Fechete, O. Conradi, A. Graichen, D. Anokhin, D.A. Ivanov, M. Moller, Int. J. Hydrog. Energy 37 (2012) 14454–14462.
[25] T. Matsushita, A. Kuze, R. Kawai., M. Hieda, N. Wada, J. Low Temp. Phys. 171 (2013) 657–663.
[26] M. Tang, Y. Hong, Z. Gu, Y. Zhang, X. Cai, Starch/Stärke 65 (2013) 702–708.
[27] C. D'Agostino, T. Kotionova, J. Mitchell, P.J. Miedziak, D.W. Knight, S.H. Taylor, G.J. Hutchings, L.F. Gladden, M.D. Mantle, Chem. Eur. J. 19 (2013) 11725–11732.

[28] T.M. Kawakami, M. Kizuki, H. Takeuchi, Y. Shibutani, Analyst 136 (2011) 897–900.
[29] J.G Powles, J.H. Strange, Proc. Phys. Soc. 82 (1963) 6–15.
[30] H.Y. Carr, E.M. Purcell, Phys. Rev. 94 (1954) 630–638.
[31] S. Meiboom, D. Gill, Rev. Sci. Instrum. 29 (1958) 688–691.
[32] Y. Urahama, M. Sasaki, Y. Kato, K. Ito, Y. Nakamura, H.J. Kishi, Adhes. Soc. Jpn. 47 (2011) 46–52.
[33] S. Yajima, K. Tohda, P. Bühlmann, Y. Umezawa, Anal. Chem. 69 (1997) 1919–1924.
[34] H. Serizawa, M. Ito, T. Kanamoto, K. Tanaka, A. Nomura, Polym. J. 14 (1982) 149–154.
[35] C.W. Davies, J. Chem. Soc. (1938) 2093–2098.
[36] L.G. Krauskopf, in: H. Zweifel, R.D. Maier, M. Schiller (Eds.), Plastics Additives Handbook, 6th edition,Hanser Publishers, Munich, 2009, p. 485 (Chapter 3.13).
[37] Y. Urahama, J. Adhes. Soc. Jpn. 46 (2010) 53–62.